Intercomponent Electronic Energy Transfer in Heteropolynuclear Complexes Containing Ruthenium- and Rhenium-Based Chromophores Bridged by an Asymmetric Quaterpyridine Ligand

Rosemary L. Cleary,[1a] Kate J. Byrom,[1a] David A. Bardwell,[1a] John C. Jeffery,[1a] Michael D. Ward,*[,1a] Giuseppe Calogero,[1b] Nicola Armaroli,[1b] Lucia Flamigni,[1b] and Francesco Barigelletti*[,1b]

University of Bristol, School of Chemistry, Cantock's Close, Bristol BS8 1TS, U.K., and Istituto FRAE-CNR, Via P. Gobetti 101, 40129 Bologna, Italy

Received December 27, 1996[⊗]

We have prepared the mononuclear complexes $[Ru(bpy)_2(AB)][PF_6]_2$, $[Ru(bpy)(AB)_2][PF_6]_2$, and $[Ru(AB)_3][PF_6]_2$ (designated **Ru**−**AB**, **Ru**−**AB$_2$**, and **Ru**−**AB$_3$**, respectively) [where bpy is 2,2′-bipyridine and **AB** is the asymmetric bis(bipyridyl) bridging ligand 2,2′:3′,2″:6″,2‴-quaterpyridine] in which there are one, two, or three (respectively) bpy-type fragments pendant from the $\{Ru(bpy)_3\}^{2+}$ core. In every case the less hindered site A of the ligand **AB** is coordinated to Ru(II) and the more hindered site B is pendant. Reaction with $Re(CO)_5Cl$ affords the heteronuclear complexes $[Ru(bpy)_2\{ABRe(CO)_3Cl\}][PF_6]_2$, $[Ru(bpy)\{ABRe(CO)_3Cl\}_2][PF_6]_2$, and $[Ru\{ABRe(CO)_3Cl\}_3][PF_6]_2$ (designated **Ru**−**ABRe**, **Ru**−**ABRe$_2$**, and **Ru**−**ABRe$_3$**, respectively) in which each pendant site B is now coordinated to a $\{Re(CO)_3Cl\}$ fragment. Because of the conformational properties of the **AB** ligand, in the tetranuclear **Ru**−**ABRe$_3$** complex the Ru-based chromophore occupies an internal position in a sort of molecular ball, the three Re-based groups being located outside. Electrochemical studies show that the pendant $\{Re(CO)_3Cl\}$ fragments exert an electron-withdrawing effect on the $\{Ru(bpy)_3\}^{2+}$ core such that the Ru(II)/Ru(III) redox couple moves to more positive potentials as the number of pendant $\{Re(CO)_3Cl\}$ fragments increases. We employed steady-state and time-resolved luminescence spectroscopy to investigate the Re → Ru intercomponent energy transfer taking place in the mixed-metal complexes and found that Re → Ru energy transfer takes place with 100% efficiency in all cases. For the tetranuclear complex, it is thus possible to convey a substantial portion of the electronic excitation energy from the molecular periphery to the center. It is also found that the peripheral Re-containing units exert a shielding effect against luminescence quenching processes at the Ru center by molecular oxygen dissolved in the solvent. During the syntheses, the unexpected byproduct $[Ru(AB)(\eta^3\text{-AB})Cl][PF_6]$ was also isolated in which one of the **AB** ligands is coordinated in a hitherto unseen terdentate mode; this was crystallographically characterized. Data for $[Ru(AB)(\eta^3\text{-AB})Cl][PF_6]\cdot 2MeCN$: $C_{44}H_{34}ClF_6N_{10}PRu$; triclinic, $P\bar{1}$; $a = 10.578(3)$ Å, $b = 14.330(2)$ Å, $c = 14.761(3)$ Å; $\alpha = 84.56(2)°$, $\beta = 70.408(12)°$, $\gamma = 86.03(2)°$; $V = 2096.8(8)$ Å^3; $Z = 2$.

Introduction

The design of multicomponent systems containing electroactive and photoactive units has attracted the attention of many research groups.[2] In these multicomponent systems, the active units are linked *via* covalent bonds and a great variety of organic or inorganic active units can be employed.[3] The field has progressively expanded and has become part of supramolecular chemistry, which also includes organized systems where receptor and substrate units are held together by weak intercomponent forces.[4,5] In the presence of suitable spatial organization for the components and properly arranged energy gradients for the occurrence of photoinduced processes,[2] the assembling of photoactive units in large arrays may lead to the implementation of useful functionalities. For instance, in favorable cases it is possible to develop photochemical molecular devices (PMDs)[6] which can perform light energy collection,[8] long-distance electronic energy transfer,[9] and charge separation,[10] or can act as sensors of the molecular environmemt through the "readibility" of their luminescence properties.[11]

Many multicomponent systems incorporating photoactive and electroactive units based on d^6 metal transition complexes have been constructed based on the attractive electrochemical and

⊗ Abstract published in *Advance ACS Abstracts,* May 15, 1997.

(1) (a) University of Bristol, School of Chemistry, Cantock's Close, Bristol BS8 1TS, UK. (b) Istituto FRAE-CNR, Via P. Gobetti 101, 40129 Bologna, Italy.

(2) (a) Gust, D., Moore, T. A., Eds. *Tetrahedron* (Special Issue No. 15) **1989**, *45*. (b) Fox, M. A., Chanon, M., Eds. *Photoinduced Electron Transfer*; Elsevier: New York, 1988; Parts A−D. (c) Mattay, J., Ed. *Top. Curr. Chem.* **1990**, *156*; **1990**, *158*; **1991**, *159*. (d) Balzani, V., De Cola, L., Eds. *Supramolecular Chemistry*; Kluwer: Dordrecht, 1992. (e) Dürr, H., Bouas-Laurent, E., Eds. *Photochromism. Molecules and Systems*; Elsevier: Amsterdam, 1990. (f) Schneider, J., Dürr, H., Eds. *Frontiers in Supramolecular Organic Chemistry and Photochemistry;* VCH: Weinheim, 1990. (g) Fabbrizzi, L., Poggi, A., Eds. *Transition Metals in Supramolecular Chemistry*; Kluwer: Dordrecht, 1994.

(3) Balzani, V.; Scandola, F. *Supramolecular Photochemistry*; Horwood: Chichester, 1991.

(4) Lehn, J.-M. *Supramolecular Chemistry*; VCH: Weinheim, 1995.

(5) Vögtle, F. *Supramolecular Chemistry*; Wiley: New York, 1991.

(6) Reference 3, Chapter 12. For a review covering photoinduced processes in polynuclear complexes, see ref 7. A selection of recent papers dealing with photoinduced processes in polynuclear complexes is listed in refs 8−10.

(7) Scandola, F.; Indelli, M. T.; Chiorboli, C.; Bignozzi, C. A. *Top. Curr. Chem.* **1990**, *158*, 63.

(8) Denti, F.; Campagna, S.; Balzani, V. In *Mesomolecules: From Molecules to Materials*; Mendenhall, G. D., Greenberg, A., Liebemann, Eds.; Chapman and Hall: New York, 1995; Chapter 3 and references therein.

(9) (a) Harriman, A.; Ziessel, R. *Chem. Commun. (Cambridge)* **1996**, 1707. (b) Barigelletti, F.; Flamigni, L.; Balzani, V.; Collin, J.-P.; Sauvage, J.-P.; Sour, A.; Constable, E. C.; Cargill Thompson, A. M. W. *J. Am. Chem. Soc.* **1994**, *116*, 7692.

S0020-1669(96)01528-5 CCC: $14.00

excited-state properties of polypyridine complexes of ruthenium(II)[12] and osmium(II).[13] In these systems the six coordination positions can be occupied by three bidentate ligands like bpy and phen, or by two tridentate ligands like tpy (bpy is 2,2′-bipyridine, phen is 1,10-phenanthroline, and tpy is 2,2′:6′,2″-terpyridine). The use of tpy-type coordination for Ru(II) and Os(II) metal ions offers important geometrical advantages;[14] for instance it is possible to construct linear and rigid arrays for vectorial transfer of energy.[9,14,15] However, if strongly luminescent systems are required, then bpy (or phen) coordination is preferred because of the outstanding luminescence properties of their Ru(II)- or Os(II)-based chromophores.[7,12,13,16]

Whereas for the building up of dinuclear species a wide variety of ditopic connecting units, including flexible and rigid spacers,[7,14−17] has been employed, for the preparation of higher nuclearity species a smaller range of bridging units is available, mostly of the dpp type [dpp is 2,3-bis(dipyridyl)pyrazine or 2,5-bis(dipyridyl)pyrazine][16] which contain two bidentate bpy-type compartments. Recently very high nuclearity species have been developed, based on Ru(II) and Os(II) centers connected by dpp bridges, that exhibit nuclear configurations of the dendrimer type.[8,16,18] Owing to the strong intercenter electronic coupling allowed by the bridging units, these dendrimer species perform as efficient light-harvesting systems capable of driving light energy to the lowest energy position, usually an Os(II) center.

The heteronuclear complexes reported here employ Ru(II)[12] and Re(I)[19] centers, connected by the asymmetric 2,2′:3′,2″:6″,2‴-quaterpyridine, **AB**,[20] Chart 1. The two chelating sites are sterically inequivalent, and the metal centers exhibit site-dependent spectroscopic and electrochemical properties, as shown in our previous studies dealing with Ru/Os[21] and Ru/Re[22] dinuclear species. In these dinuclear species, the **AB** ditopic ligand holds the metal centers relatively close each other, $d_{MM} \approx 7-8$ Å, and X-ray results have shown that "stacking" involving a bpy subunit of one **AB** bridging ligand and one coordinated bpy ligand of $[(bpy)_2Os(AB)Ru(bpy)_2]^{2+}$ takes place,[21] resulting in strong intermetal electronic coupling. In order to study the energy transfer processes involving the various components, we have prepared the following heteronuclear complexes: $[Ru(bpy)_2\{ABRe(CO)_3Cl\}]^{2+}$, $[Ru(bpy)\{ABRe(CO)_3Cl\}_2]^{2+}$, and $[Ru\{ABRe(CO)_3Cl\}_3]^{2+}$ (designated **Ru**−**ABRe, Ru**−**ABRe$_2$**, and **Ru**−**ABRe$_3$**, respectively) in which one, two, or three Re(I) centers are pendant from a $\{Ru(bpy)_3\}^{2+}$-type core, together with their mononuclear Ru(II) counterparts $[Ru(bpy)_2(AB)]^{2+}$, $[Ru(bpy)(AB)_2]^{2+}$, and $[Ru(AB)_3]^{2+}$ (designated **Ru**−**AB**,[21] **Ru**−**AB$_2$**, and **Ru**−**AB$_3$**, respectively), as hexafluorophosphate salts (Chart 1). We report here the syntheses, characterization, and electrochemical properties of these complexes, together with their spectroscopic properties (absorption spectra, emission spectra, and luminescence lifetimes).

Experimental Section

Materials and Synthetic Procedures. Ruthenium trichloride hydrate and $Re(CO)_5Cl$ were purchased from Johnson Matthey and used as received. Ligand **AB**,[20,22] complexes **Ru**−**AB** and **Ru**−**ABRe**,[22] and $[Ru(bpy)_2Cl_2]$[23] were prepared as previously described.

$Ru(AB)_2Cl_2$. This was prepared according to the method used for $[Ru(bpy)_2Cl_2]$.[23] A mixture of commercial hydrated ruthenium trichloride (0.116 g, 0.48 mmol), **AB** (0.300 g, 0.96 mmol), and LiCl (0.17 g, 4 mmol) was heated to reflux in DMF (30 cm^3) for 6 h under N_2 to afford a deep purple solution. After evaporation to dryness, the mixture was purified by chromatography on alumina using CH_2Cl_2/MeOH (95:5, v/v). Yield: 0.130 g (34%). ESMS: m/z = 757 $[M - Cl]^+$, 361 $[M - 2Cl]^{2+}$.

$[Ru(AB)_2(bpy)][PF_6]_2$. A mixture of $Ru(AB)_2Cl_2$ (0.100 g, 1.3 mmol) and bpy (0.021 g, 1.3 mmol) was heated to reflux in EtOH for 4 h to afford an orange solution. On addition of aqueous KPF_6 an orange solid precipitated, which was filtered off and dried. The crude

(10) (a) Indelli, M. T.; Bignozzi, C. A.; Harriman, A.; Schoonover, J. R.; Scandola, F. *J. Am. Chem. Soc.* **1994**, *116*, 3768. (b) Sutter, J.-P.; Grove, D. M.; Beley, M.; Collin, J.-P.; Veldman, N.; Spek, A. L.; Sauvage, J.-P.; van Koten, G. *Angew. Chem., Int. Ed. Engl.* **1994**, *33*, 1282. (c) Tan-Sien-Hee, L.; Kirsch-De Mesmaeker, A. *J. Chem. Soc., Dalton Trans.* **1994**, 3651. (d) Slone, R. V.; Yoon, D. I.; Calhoun, R. M.; Hupp, J. T. *J. Am. Chem. Soc.* **1995**, *117*, 11813. (e) Baba, A. I.; Ensley, H. E.; Schmehl, R. H. *Inorg. Chem.* **1995**, *34*, 1198. (f) Argazzi, R.; Bignozzi, C. A. *J. Am. Chem. Soc.* **1995**, *117*, 11815. (g) Larson, S. L.; Elliott, C. M; Kelley, D. F. *J. Phys. Chem.* **1995**, *99*, 6530. (h) Chau, D. E. K.-Y., James, B. R. *Inorg. Chim. Acta* **1995**, *240*, 419. (i) Kropf, M.; Joselevich, E., Dürr, H.; Willner, I. *J. Am. Chem. Soc.* **1996**, *118*, 655. (j) Wilson, G. J.; Sasse, W. H. F.; Mau, A. W.-H. *Chem. Phys. Lett.* **1996**, *250*, 583. (k) Milkewich, M.; Brauns, E.; Brewer, K. J. *Inorg. Chem.* **1996**, *35*, 1737. (l) Indelli, M. T.; Scandola, F.; Collin, J.-P., Sauvage, J.-P.; Sour, A. *Inorg. Chem.* **1996**, *35*, 302. (m) Vogler, L. M.; Brewer, K. J. *Inorg. Chem.* **1996**, *35*, 818. (n) Bolger, J.; Gourdon, A.; Ishow, E.; Launay, J.-P. *Inorg. Chem.* **1996**, *35*, 2937. (o) Haga, M.-a.; Ali, Md. M.; Koseki, S.; Fujimoto, K.; Yoshimura, A.; Nozaki, K.; Ohno, T.; Nakajima, K.; Stufkens, D. J. *Inorg. Chem.* **1996**, *35*, 3335.

(11) (a) Bissel, R. A.; De Silva, A. P.; Gunaratne, H. Q. N.; Lynch, P. L. M.; Maguire, G. E. M.; Sandanayake, K. R. A. S. *Chem. Soc. Rev.* **1992**, *21*, 187. (b) Fabbrizzi, L.; Licchelli, M.; Pallavicini, P.; Perotto, A.; Taglietti, A.; Sacchi, D. *Chem. Eur. J.* **1996**, *2*, 75. (c) Beer, P. D. *Chem. Commun. (Cambridge)* **1996**, 689.

(12) (a) Meyer, T. J. *Pure Appl. Chem.* **1986**, *58*, 1193. (b) Juris, A.; Balzani, V.; Barigelletti, F.; Campagna, S.; Belser, P.; von Zelewsky, A. *Coord. Chem. Rev.* **1988**, *84*, 85. (c) Meyer, T. J. *Acc. Chem. Res.* **1989**, *22*, 163. (d) Kalyanasundaram, K. *Photochemistry of Polypyridine and Porphyrin Complexes*; Academic Press: London, 1991.

(13) (a) Kober, E. M.; Caspar, J. V.; Sullivan, B. P.; Meyer, T. J. *Inorg. Chem.* **1988**, *27*, 4587. (b) Brewer, R. G.; Jensen, G. E.; Brewer, K. J. *Inorg. Chem.* **1994**, *33*, 124.

(14) Sauvage, J.-P.; Collin, J.-P.; Chambron, J.-C.; Guillerez, S.; Coudret, C.; Balzani, V.; Barigelletti, F.; De Cola, L.; Flamigni, L. *Chem. Rev.* **1994**, *94*, 993.

(15) (a) Barigelletti, F.; Flamigni, L.; Collin, J.-P.; Sauvage, J.-P. *Chem. Commun. (Cambridge)* **1997**, 333. (b) Constable, E. C. *Prog. Inorg. Chem.* **1994**, *42*, 67. (c) Constable, E. C.; Cargill Thompson, A. M. W. *New J. Chem.* **1996**, *20*, 65.

(16) Balzani, V.; Juris, A.; Venturi, M.; Campagna, S.; Serroni, S. *Chem. Rev.* **1996**, *96*, 759.

(17) (a) Barigelletti, F.; Flamigni, L.; Guardigli, M.; Juris, A.; Beley, M; Chodorowski-Kimmes, S.; Collin, J.-P.; Sauvage, J.-P. *Inorg. Chem.* **1996**, *35*, 136. (b) De Cola, L.; Balzani, V.; Barigelletti, F.; Flamigni, L.; Belser, P.; von Zelewsky, A.; Frank, M.; Vögtle, F. *Inorg. Chem.* **1993**, *32*, 5228. (c) Vögtle, F.; Frank, M.; Nieger, M.; Belser, P.; von Zelewsky, A.; Balzani, V.; Barigelletti, F.; De Cola, L.; Flamigni, L. *Angew. Chem., Int. Ed. Engl.* **1993**, *32*, 1643. (d) Benniston, A. C.; Grosshenny, V.; Harriman, A.; Ziessel, R. *Angew. Chem., Int. Ed. Engl.* **1994**, *33*, 1884. (e) Benniston, A. C.; Goulle, V.; Harriman, A.; Lehn, J.-M.; Marczinke, B. *J. Phys. Chem.* **1994**, *98*, 7798.

(18) Denti, G.; Campagna, S.; Serroni, S.; Ciano, M.; Balzani, V. *J. Am. Chem. Soc.* **1992**, *114*, 2944.

(19) (a) Juris, A.; Campagna, S.; Bidd, I.; Lehn, J.-M.; Ziessel, R. *Inorg. Chem.* **1988**, *27*, 4007. (b) Worl, L. A.; Duesing, R.; Chen, P.; Della Ciana, L.; Meyer, T. J. *J. Chem. Soc., Dalton Trans.* **1991**, 849. (c) Schanze, S. K; MacQueen, D. B.; Perkins, T. A.; Cabana, L. A. *Coord. Chem. Rev.* **1993**, *122*, 63. (d) Wallace, L.; Rillema, D. P. *Inorg. Chem.* **1993**, *32*, 3843. (e) Sacksteder, L.; Lee, M.; Demas, J. N.; DeGraff, B. A. *J. Am. Chem. Soc.* **1993**, *115*, 8230. (f) Thornton, N. B.; Schanze, K. S. *Inorg. Chem.* **1993**, *32*, 4994. (g) Wang, Y.; Hauser, B. T.; Rooney, M. M.; Burton, R. D.; Schanze, K. S. *J. Am. Chem. Soc.* **1993**, *115*, 5675. (h) Spellane, P.; Watts, R. J.; Vogler, A. *Inorg. Chem.* **1993**, *32*, 5633. (i) Kotch, T. G.; Lees, A. J.; Fuerniss, S. J.; Papathomas, K. I.; Snyder, R. W. *Inorg. Chem.* **1993**, *32*, 2570. (j) Zipp, A. P.; Sacksteder, L.; Streich, J.; Cook, A.; Demas, J. N.; DeGraff, B. A. *Inorg. Chem.* **1993**, *32*, 5629. (k) Lee, Y. F.; Kirchhoff, J. R. *J. Am. Chem. Soc.* **1994**, *116*, 3599. (l) Wang, Y.; Schanze, K. S. *Inorg. Chem.* **1994**, *33*, 1354.

(20) Ward, M. D. *J. Chem. Soc., Dalton Trans.* **1993**, 1321.

(21) Balzani, V.; Bardwell, D. A.; Barigelletti, F.; Cleary, R. L.; Guardigli, M.; Jeffery, J. C.; Sovrani, T.; Ward, M. D. *J. Chem. Soc., Dalton Trans.* **1995**, 3601.

(22) Bardwell, D. A.; Barigelletti, F.; Cleary, R. L.; Flamigni, L.; Guardigli, M.; Jeffery, J. C.; Ward, M. D. *Inorg. Chem.* **1995**, *34*, 2438.

(23) Sullivan, B. P.; Salmon, D. J.; Meyer, T. J. *Inorg. Chem.* **1978**, *17*, 3334.

Chart 1. The Ligand **AB** and the Investigated Complexes

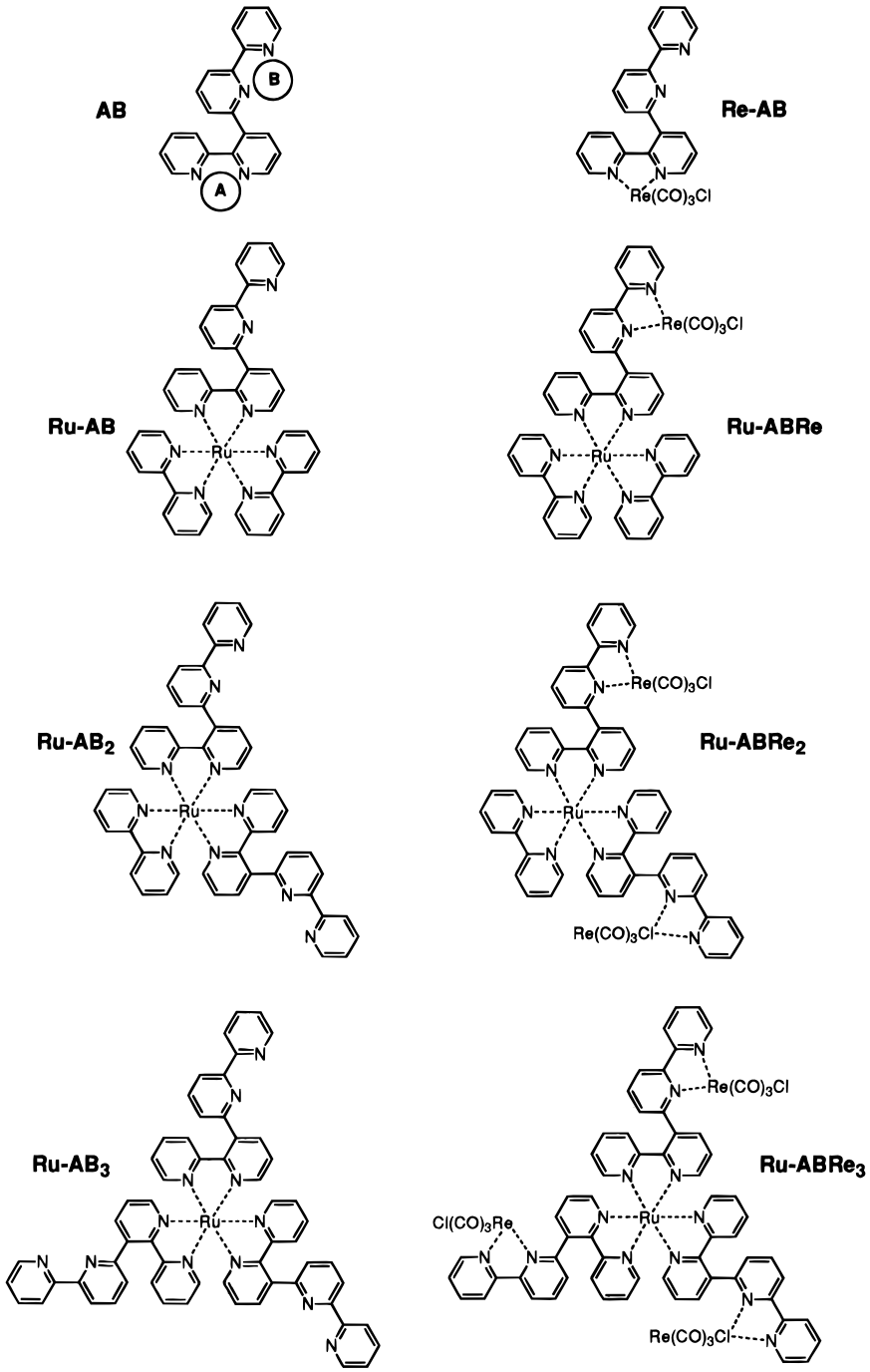

product was purified by chromatography on alumina using MeCN/toluene (2:1, v/v). Yield: 0.045 g (30%). ESMS: $m/z = 1023$ [M − PF_6]$^+$, 439 [M − $2PF_6$]$^{2+}$.

[Ru(AB)$_3$][PF$_6$]$_2$ and [Ru(AB)(η^3-AB)Cl][PF$_6$]. A mixture of commercial hydrated ruthenium trichloride (0.100 g, 0.41 mmol) and **AB** (0.430 g, 1.39 mmol) in ethylene glycol (20 cm^3) was heated to reflux for 1 h to afford an orange solution. On cooling followed by addition of aqueous KPF_6 a dark orange solid precipitated. TLC analysis [silica, MeCN/H_2O/saturated aqueous KNO_3 (14:2:1, v/v)] showed a slow-moving major orange component and a trace amount of a fast-moving purple byproduct. These were readily separated by column chromatography [silica, MeCN/H_2O/saturated aqueous KNO_3 (14:2:1, v/v)]. The combined fractions of each pure material were concentrated *in vacuo*, and the complex was precipitated by addition of KPF_6. For [Ru(AB)$_3$][PF$_6$]$_2$, which was present in substantial amounts, the pure solid was filtered off and dried; giving a yield of 0.430 g (79%). For [Ru(AB)(η^3-AB)Cl][PF$_6$], which was present in trace amounts, the suspension was extracted with a small volume of CH_2Cl_2 to afford a purple solution, which was evaporated to dryness to give 0.018 g (5%). ESMS of [Ru(AB)$_3$][PF$_6$]$_2$: $m/z = 1177$ [M − PF_6]$^+$, 515 [M − $2PF_6$]$^{2+}$. ESMS of [Ru(AB)(η^3-AB)Cl][PF$_6$]: 757 [M − PF_6]$^+$, 722 [M − Cl − PF_6]$^+$.

[Ru(bpy){ABRe(CO)$_3$Cl}$_2$][PF$_6$]$_2$ (Ru−ABRe$_2$). A mixture of [Ru(AB)$_2$(bpy)][PF$_6$]$_2$ (0.050 g, 0.43 mmol) and $Re(CO)_5Cl$ (0.062 g, 1.71 mmol) in DMF was heated to 125 °C with stirring for 3 days. After evaporation of the solvent *in vacuo*, the residue was purified by chromatography on silica using a mixture of MeCN/H_2O/saturated aqueous KNO_3 (14:2:1, v/v), as described above. Yield: 0.035 g, 46%. ESMS: $m/z = 744$ [M − $2PF_6$]$^{2+}$.

[Ru{ABRe(CO)$_3$Cl}$_3$][PF$_6$]$_2$ (Ru−ABRe$_3$). A mixture of [Ru(AB)$_3$]-[PF$_6$]$_2$ (0.100 g, 0.076 mmol) and $Re(CO)_5Cl$ (0.163 g, 0.45 mmol) in DMF was heated to 125 °C with stirring for 3 days. After evaporation of the solvent *in vacuo*, the residue was purified by chromatography on silica using a mixture of MeCN/H_2O/saturated aqueous KNO_3 (14:2:1, v/v), as described above. Yield: 0.066 g (42%). ESMS: $m/z = 975$ [M − $2PF_6$]$^{2+}$.

Satisfactory elemental analyses of all new complexes were obtained.

Equipment and Methods. ^{1}H NMR spectra were recorded on Jeol GX270 or Lambda 300 spectrometers. Fast atom bombardment (FAB) mass spectra were recorded on a VG Autospec instrument, with 3-nitrobenzyl alcohol as matrix. Electrospray mass spectra were performed with MeCN solutions of the complexes on a VG Quattro instrument. Electrochemical measurements were made with a PC-controlled EG&G/PAR 273A potentiostat, using platinum bead working and auxiliary electrodes, and an SCE reference electrode. The measurements were performed using acetonitrile distilled over calcium hydride, with 0.1 mol dm^{-3} [NBu$^n_4$][PF$_6$] as supporting electrolyte. Ferrocene was added at the end of each experiment as an internal reference, and all redox potentials are quoted *vs* the ferrocene/ferrocenium couple (Fc/Fc$^+$).

Ground-state absorption spectra were obtained in DMF/CH_2Cl_2 (9:1, v/v) solutions on a Perkin-Elmer Lambda 9 spectrophotometer. Luminescence experiments were performed in the same solvent both at room temperature and at 77 K. When necessary, solutions were degassed either by bubbling Ar for 10 min or by evacuating the air *via* repeated freeze−pump−thaw cycles. Uncorrected luminescence spectra were obtained with a Spex Fluorolog II spectrofluorimeter, and uncorrected band maxima are used throughout. Correction of the luminescence intensity profile was done according to previously described procedures.[22] Luminescence quantum yields Φ_s were evaluated by comparing areas under the corrected luminescence spectra on an energy scale and according to the following equation:

$$\Phi_s = \frac{A_r n_s^2 (\text{area})_s}{A_s n_r^2 (\text{area})_r} \quad (1)$$

where A is the absorbance, n is the refractive index of the solvent employed (taken as a compositional average for DMF/CH_2Cl_2, 9:1, v/v), and s and r stand for sample and reference, respectively. The reference compound was [Ru(bpy)$_3$]Cl$_2$ in air-equilibrated water ($\Phi = 0.028$).[24] Absorbance values were ≤ 0.1 at the employed excitation wavelength, $\lambda = 380$ and 465 nm. Luminescence lifetimes were obtained with IBH single-photon equipment.[22] The solutions of all complexes were stable over several days. The experimental uncertainty in the band maximum for absorption and luminescence spectra is 2 nm; that for luminescence intensity is 20%. The time resolution of the single-photon spectrometer is 200 ps, and the uncertainty on the evaluated lifetimes is 8%.

Crystal Structure of [Ru(AB)(η^3-AB)Cl][PF$_6$]·2MeCN. Recrystallization of [Ru(AB)(η^3-AB)Cl][PF$_6$] by diffusion of ether vapor into a concentrated acetonitrile solution of the complex afforded purple block-like crystals of [Ru(AB)(η^3-AB)Cl][PF$_6$]·2MeCN. A suitable crystal (dimensions 0.5 × 0.4 × 0.2 mm^3) was coated with paraffin oil and mounted on a glass fiber under a stream of cold N_2 (−100 °C). Data were collected using a Siemens SMART three-circle diffractometer with a CCD area detector (graphite-monochromatized Mo K$_\alpha$ X-radiation, $\bar{\lambda} = 0.710\ 73$ Å); 10014 data were collected to $2\theta_{max} = 50°$, which gave, after merging, 7140 unique data with $R_{int} = 0.026$. Data were corrected for Lorentz and polarization effects, and for absorption effects by an empirical method based on multiple measurements of equivalent data. Details of the crystal parameters, data collection, and refinement are in Table 1. The structure was solved by conventional direct methods (SHELXTL) and refined by the full-matrix least-squares method on all F^2 data (SHELX93) using a Silicon Graphics Indy computer.[25] All non-hydrogen atoms were refined anisotropically; hydrogen atoms were included in calculated positions and refined with isotropic thermal parameters. Selected bond lengths and angles are in Table 2.

Table 1. Crystallographic Data for [Ru(AB)(η^3-AB)Cl][PF$_6$]·2MeCN

empirical formula	$C_{44}H_{34}ClF_6N_{10}PRu$
fw	984.30
space group	$P\bar{1}$
a, Å	10.578(3)
b, Å	14.330(2)
c, Å	14.761(3)
α, deg	84.56(2)
β, deg	70.408(12)
γ, deg	86.03(2)
V, Å^3	2096.8(8)
Z	2
ρ_{calc}, g cm^{-3}	1.559
μ, mm^{-1}	0.549
T, K	173(2)
λ, Å	0.710 73
R1, wR2[a,b]	0.046, 0.104

[a] Structure was refined on F_o^2 using all data; the value of R1 is given for comparison with older refinements based on F_o with a typical threshold of $F \geq 4\sigma(F)$. [b] $wR2 = [\sum[w(F_o^2 - F_c^2)^2]/\sum w(F_o^2)^2]^{1/2}$ where $w^{-1} = [\sigma^2(F_o^2) + (aP)^2 + bP]$ and $P = [\max(F_o^2,0) + 2F_c^2]/3$; the weighting factors are $a = 0.0032$, $b = 5.6841$.

Table 2. Selected Bond Lengths (Å) and Angles (deg) for [Ru(AB)(η^3-AB)Cl][PF$_6$]·2MeCN

Ru(1)−N(81)	2.043(3)	Ru(1)−N(21)	2.052(3)
Ru(1)−N(71)	2.055(3)	Ru(1)−N(11)	2.059(3)
Ru(1)−N(41)	2.112(3)	Ru(1)−Cl(1)	2.4073(11)

N(21)−Ru(1)−N(81)	89.30(12)	N(71)−Ru(1)−N(81)	77.68(12)
N(21)−Ru(1)−N(71)	99.89(12)	N(11)−Ru(1)−N(81)	89.75(12)
N(21)−Ru(1)−N(11)	78.39(13)	N(71)−Ru(1)−N(11)	167.36(12)
N(41)−Ru(1)−N(81)	173.11(13)	N(21)−Ru(1)−N(41)	85.23(12)
N(41)−Ru(1)−N(71)	99.11(12)	N(11)−Ru(1)−N(41)	93.24(12)
N(81)−Ru(1)−Cl(1)	92.77(9)	N(21)−Ru(1)−Cl(1)	172.56(9)
N(71)−Ru(1)−Cl(1)	87.54(9)	N(11)−Ru(1)−Cl(1)	94.46(10)
N(41)−Ru(1)−Cl(1)	93.18(9)		

Results

Syntheses and Characterization of Mononuclear Ru and Polynuclear Ru/Re Complexes. The series of complexes described here (Chart 1) contain one, two, or three {Re(bpy)(CO)$_3$Cl} chromophores pendant from a {Ru(bpy)$_3$}$^{2+}$-type core. To prepare these we needed mononuclear Ru(II) complexes wth one, two, or three pendant bpy-type binding sites, which necessitated prior preparation of [Ru(bpy)$_2$(AB)]$^{2+}$, [Ru(bpy)(AB)$_2$]$^{2+}$, and [Ru(AB)$_3$]$^{2+}$, in which the **AB** ligand is coordinated to Ru(II) by the A site and the B site is pendant. This is the normal mode of coordination of **AB** to a single metal center because site A is much less sterically hindered than site B. Of these complexes [Ru(bpy)$_2$(AB)]$^{2+}$ has been described before.[20−22] The homoleptic complex [Ru(AB)$_3$]$^{2+}$ was simply prepared by reaction of 3 equiv of the free ligand **AB** with ruthenium trichloride. Synthesis of [Ru(bpy)(AB)$_2$]$^{2+}$ required initial preparation of [Ru(AB)$_2$Cl$_2$], by the same route that is commonly used for preparation of [Ru(bpy)$_2$Cl$_2$], *i.e.*, reaction of **AB** with ruthenium trichloride in a 2:1 ratio in DMF in the presence of a large excess of LiCl. Subsequent reaction of [Ru(AB)$_2$Cl$_2$] with 1 equiv of bpy then afforded [Ru(bpy)(AB)$_2$]$^{2+}$. Prolonged reaction of each of these with a stoichiometric excess of [Re(CO)$_5$Cl] (typically 2 equiv per binding site to be occupied) in DMF at 125 °C then afforded the mixed-metal Ru/Re complexes, which could be purified chromatographically. Although each complex can consist of several diastereoisomeric forms (each individual metal center is chiral), these did not separate during chromatography.

The main characterizational tool was electrospray mass spectrometry. In the last few years this has become a popular tool for the characterization of high-nuclearity and/or highly charged coordination complexes.[26] The principal mass spectral peaks (see Experimental Section) in every case confirm the formulations of the complexes. Generally, loss of both hexaflu-

(24) Nakamaru, K. *Bull. Chem. Soc. Jpn.* **1982**, *55*, 2697.
(25) *SHELXTL program system*, version 5.03; Siemens Analytical X-ray Instruments: Madison, WI, 1995.
(26) Przybylski, M.; Glocker, M. O. *Angew. Chem., Int. Ed. Engl.* **1996**, *35*, 807.

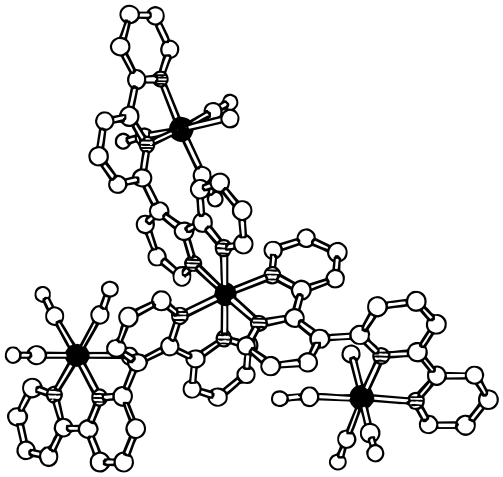

Figure 1. Computed minimum-energy structure of the complex cation of **Ru−ABRe$_3$**. The metal atoms are black; the nitrogen atoms are shaded.

orophosphate anions was observed, giving a doubly-charged fragment which appeared therefore at the *m/z* value corresponding to half of the value that would be expected for a +1 fragment.

We were unable to obtain crystals of **Ru−ABRe$_2$** and **Ru−ABRe$_3$**, but the computed structure of the **Ru−ABRe$_3$** dication (from a molecular mechanics energy minimization calculation using MM2 parameters, on a CAChe workstation) is shown in Figure 1. The geometrical arrangement of **AB** ligands around the Ru(II) center was assumed to be the more sterically favorable meridional (rather than facial) isomer. The configurations of the (chiral) Re centers are arbitrary; it was found that no significant differences in gross structure or the energy of the complex arose between different diastereoisomers, probably because the Re centers are quite far apart from one another. The computed structure shows that each of the **AB** bridging ligands has the two bpy fragments perpendicular, as expected: the crystal structures of $[(CO)_3ClRe(AB)Ru(bpy)_2][PF_6]_2\cdot 2MeCN\cdot 0.5Et_2O$[22] and $[(bpy)_2Os(AB)Ru(bpy)][PF_6]_4\cdot 3MeCN$[21] show that coordination at the B site results in a nearly perpendicular arrangement for the two A and B halves of the bridging ligand for steric reasons, compared to an angle of 41° between the coordinated and pendant bpy fragments of [Ru(AB)(κ^3-AB)Cl][PF_6] (below). **Ru−ABRe$_3$** therefore assumes a roughly spheroidal shape with the ruthenium ion in the center, and the three peripheral {Re(bpy)$(CO)_3$Cl} fragments afford a considerable degree of steric shielding around the ruthenium core: this point is of significance for interpretation of the luminescence results (see later).

Preparation and Crystal Structure of [Ru(AB)(η^3-AB)Cl][PF_6]·2MeCN. During preparation of the homoleptic mononuclear complex $[Ru(AB)_3]^{2+}$ we consistently observed traces of a purple material which could be separated chromatographically from the main (orange) product. Its nature was initially unclear. The ES mass spectrum indicated the presence of a monocation $[Ru(AB)_2Cl]^+$ which, if **AB** were coordinated in the normal bidentate manner, would be only five-coordinate. The elemental analysis was exactly consistent with the formulation $[Ru(AB)_2Cl][PF_6]$. Its electrochemical behavior [a reversible Ru(II)/Ru(III) couple at $E_{1/2}$ = +0.42 V *vs* Fc/Fc$^+$] was consistent with the presence of a RuN_5Cl fragment.[12b,27] The ^{1}H NMR spectrum showed the presence of 28 inequivalent aromatic protons, most of them overlapping in a poorly-resolved

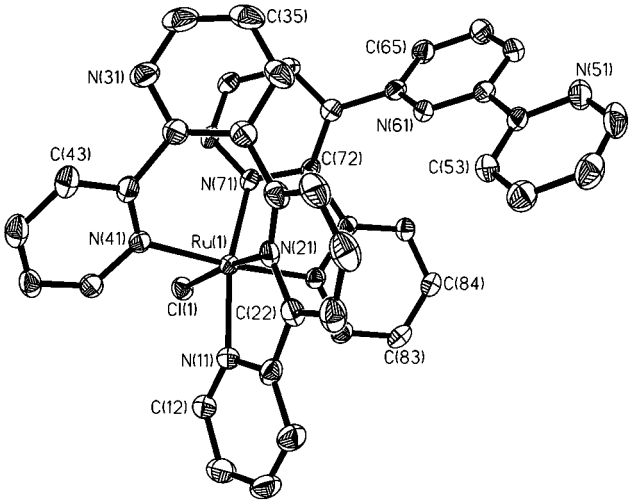

Figure 2. Crystal structure of [Ru(AB)(η^3-AB)Cl][PF_6]·2MeCN (thermal ellipsoids are at the 40% probability level).

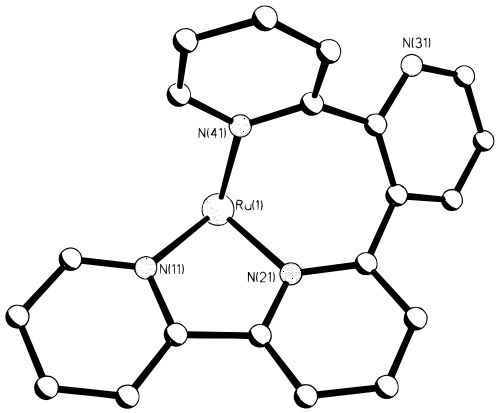

Figure 3. Fragment of the crystal structure of [Ru(AB)(η^3-AB)Cl][PF_6]·2MeCN showing the facial terdentate coordination mode of the η^3-AB ligand.

mass between 6.5 and 8.5 ppm; however, an isolated signal integrating to one proton at 10.3 ppm could be ascribed to a pyridyl H^6 proton which is directed toward a *cis*-chloride ligand and therefore strongly deshielded.[28]

An X-ray crystal structure determination (Figure 2, Tables 1 and 2) resolved the problem, showing that the formulation of the cation is indeed $[Ru(AB)_2Cl]^+$ but with one of the **AB** ligands coordinated in a hitherto unseen terdentate manner, *via* the more hindered binding site [site B; atoms N(11) and N(21)] and *one* of the pyridyl donors of site A [N(41)]. This is a kinetic product which arises when the more sterically hindered site B coordinates first to the kinetically inert metal center; by suitable folding of the ligand N(41) can also coordinate but N(31) cannot, giving a facial terdentate binding mode (Figure 3). The Ru−N(41) bond at 2.112(3) Å is significantly longer than the other four Ru−N bonds (2.04−2.06 Å) because of the steric constraints inherent in this unexpected mode of coordination. The mean-plane angles between adjacent pyridyl rings in this ligand are 13° between the two coordinated pyridyl rings, 53° between the central two rings [containing N(21) and N(31)], and finally 56° between the rings containing N(31) and N(41).

The second **AB** ligand is coordinated in the normal way *via* site A, in which the two rings are essentially coplanar. There

(27) Cathey, C. J.; Constable, E. C.; Hannon, M. J.; Tocher, D. A.; Ward, M. D. *J. Chem. Soc., Chem. Commun.* **1990**, 621.

(28) (a) Constable, E. C.; Hannon, M. J. *Inorg. Chim. Acta* **1993**, *211*, 101. (b) Birchall, J. D.; O'Donoghue, T. D.; Wood, J. R. *Inorg. Chim. Acta* **1979**, *37*, L461.

Table 3. Electrochemical Data

complex	$E_{1/2}$/V[a] Re(I)/Re(II)[b]	Ru(II)/Ru(III)[c]	ligand-based[d]		
Ru−AB[e]		+0.90	−1.66	−1.89	−2.12
Ru−AB$_2$		+0.90	−1.63	−1.82	−2.09
Ru−AB$_3$		+0.90	−1.63	−1.82	−2.02
[Ru(AB)(η^3-AB)Cl][PF$_6$]		+0.42	−1.74	−1.99	
Ru−ABRe[e]	+1.16	+0.93	−1.56	−1.77	−2.12
Ru−ABRe$_2$	+1.17	+0.98	−1.58	−1.78	−1.99
Ru−ABRe$_3$	+1.15	+1.04	−1.60	−1.80	−1.92

[a] All measurements made in MeCN containing 0.1 mol dm^{-3} N(^{n}Bu)$_4$PF$_6$ at a Pt working electrode, at a scan rate of 0.2 V s^{-1}. Potentials are *vs* ferrocene/ferrocenium. [b] All Re(I)/Re(II) couples were irreversible; the potentials quoted are taken from square-wave voltammograms. [c] All Ru(II)/Ru(III) couples (when resolved) were chemically reversible with ΔE_p values of typically 70−90 mV. [d] Peak potentials of ligand-based processes extracted from square-wave voltammograms. [e] From ref 22; data included for comparison purposes.

is a torsion angle of 41° between the rings containing N(61) and N(71) (*i.e.*, between the coordinated bpy fragment and the first pendant ring); the pendant bpy fragment is approximately *trans*-coplanar, with an angle of 6° between these two pyridyl rings. It is noticeable that the torsion angle between the free and coordinated bpy fragments (41°) is substantially less in this complex than in those dinuclear complexes where an additional metal fragment is coordinated at the second bpy site; in such complexes the two halves of bridging ligand **AB** are essentially perpendicular due to the additional steric bulk of the metal complex fragments coordinated at the second bpy site.[21,22]

Electrochemical Studies. The electrochemical properties of the complexes are collected in Table 3, together with the data for [Ru(bpy)$_2$(AB)][PF$_6$]$_2$ (**Ru−AB**) and [Ru(bpy)$_2$(AB)Re(CO)$_3$Cl][PF$_6$]$_2$ (**Ru−Re**) for comparison.[22] Successive substitution of bpy ligands by **AB** ligands along the series [Ru(bpy)$_x$(AB)$_y$][PF$_6$]$_2$ (x = 3, 2, 1, 0; y = 0, 1, 2, 3) has no effect on the potential of the reversible Ru(II)/Ru(III) couple, which remains at +0.90 V *vs* Fc/Fc$^+$ throughout. All of these mononuclear complexes also show three reductions at potentials characteristic of coordinated bpy fragments. In some cases the closely-spaced reductions were not clearly defined by cyclic voltammetry and the return waves were obscured by desorption spikes; the peak potentials of the ligand-based reductions were therefore taken from square-wave voltammograms.

In the mixed-metal Ru/Re complexes, separate metal-based Ru(II)/Ru(III) and Re(I)/Re(II) couples could be distinguished; a typical voltammogram is shown in Figure 4. In each case the Ru(II)/Ru(III) couple is chemically reversible (equal cathodic and anodic peak currents; peak−peak separation < 100 mV) and the Re(I)/Re(II) couple (which gives a more intense signal) is irreversible, which is consistent with the known behavior of the component Ru[12] and Re[19] fragments. The potential of the Re(I)/Re(II) couple is essentially invariant throughout the series **Ru−ABRe$_n$**, which is consistent with the fact that all of the Re fragments are in the same local environment and are too far apart from one another to interact significantly. However, addition of increasing numbers of Re substituents to the {Ru(bpy)$_3$}$^{2+}$ core results in a steady shift of the Ru(II)/Ru(III) potential from +0.90 V to +1.04 V *vs* Fc/Fc$^+$. The Re fragments are therefore weakly electron-withdrawing, despite the near-orthogonal twist between the two halves of each **AB** bridging ligand. This effect cannot be due to the presence of the B-type bpy substituents themselves, as [Ru(AB)$_3$]$^{2+}$ has the same redox potential as [Ru(bpy)$_3$]$^{2+}$; it is the attachment of {Re(CO)$_3$Cl} fragments at the pendant B sites that results in electron withdrawal from the Ru core.

Absorption Spectra. Ground-state absorption maxima for the complexes investigated are collected in Table 4. Data for the mononuclear model complex [Re(AB)(CO)$_3$Cl] (**Re−AB**) are also included for comparison purposes. We note that in

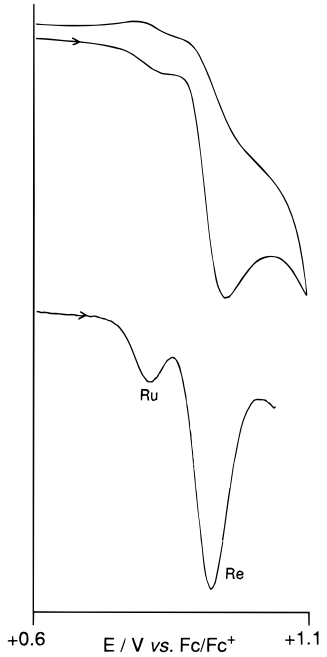

Figure 4. Cyclic (top) and square-wave (bottom) voltammograms of **Ru−ABRe$_2$** in MeCN. The Ru- and Re-based processes are labeled on the square-wave voltammogram.

Table 4. Absorption Maxima from Electronic Spectra of the New Complexes[a]

complex	λ_{max}, nm ($10^{-3}\epsilon$, M^{-1} cm^{-1})			
Ru−AB[b]	457 (14)			287 (97)
Ru−AB$_2$	463 (12)			289 (70)
Ru−AB$_3$	465 (13)			289 (73)
Ru−ABRe[b]	456 (14)	380 (sh)	330 (sh)	289 (76)
Ru−ABRe$_2$	472 (12)	380 (sh)	320 (sh)	289 (62)
Ru−ABRe$_3$	471 (19)	380 (sh)	320 (sh)	293 (75)
Re−AB[b]		378 (3.8)	320 (sh)	294 (16)
[Ru(bpy)$_3$]$^{2+}$ [c]	452 (14.6)			288 (76.6)

[a] In DMF/CH_2Cl_2 as solvent (9:1 v/v), at room temperature. [b] From ref 22. [c] Acetonitrile solvent, from ref 17b.

the mixed-metal complexes (Chart 1) coordination of the Re center occurs at the B site of **AB** quaterpyridine. In contrast, in **Re−AB**, which was previously investigated by us,[22] the metal center is coordinated to the **AB** ligand *via* the A chelating site.[29] Thus, strictly speaking, **Re−AB** is not a fully adequate reference model for the Re-based moiety of the presently investigated heteronuclear complexes, but it is the best we have. Relevant absorption features of **Re−AB** include metal-to-ligand charge

(29) For reasons discussed in ref 22, it was not possible to obtain the positional isomer Re(BA)(CO)$_3$Cl, *i.e.*, with the metal coordinated at the B site of **AB**.

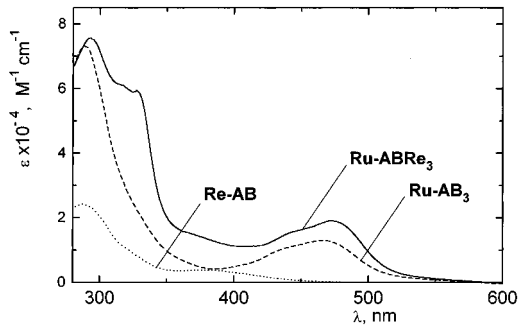

Figure 5. Absorption spectra for the **Re**−**AB**, **Ru**−**AB$_3$**, and **Ru**−**ABRe$_3$** complexes at room temperature.

transfer (MLCT, *i.e.*, Re → **AB** CT) and ligand-centered (LC) bands occurring at 378 and 294 nm, respectively.

All of the **Ru**−**AB$_n$** and **Ru**−**ABRe$_n$** complexes ($n = 1-3$) exhibit ligand-centered (^{1}LC) and metal-to-ligand charge transfer (^{1}MLCT, with the involvement of both bpy and **AB** ligands) features, with typical extinction coefficients, $\epsilon \sim 10^5$ and 10^4 M^{-1} cm^{-1}, respectively.[12] In the **Ru**−**ABRe$_n$** series of complexes both Ru → **AB** and Re → **BA** CT transitions can take place, occurring at 456−472 and ∼380 nm (as shoulders), respectively (Table 4). In particular, one sees that the energy position of the Ru → L CT maximum moves from 457 to 465 nm for the **Ru**−**AB** and **Ru**−**AB$_3$** complexes, respectively, and from 456 to 471 nm for the **Ru**−**ABRe** and **Ru**−**ABRe$_3$** complexes, respectively. This behavior is consistent with sequential substitution of the **AB** ligand and **ABRe** moiety in place of a simple bpy ligand resulting in a greater degree of delocalization for the promoted Ru → **AB** electron. It is noticeable that this electron-withdrawing effect is more pronounced in **Ru**−**ABRe$_3$** than in **Ru**−**AB$_3$**, *i.e.*, the pendant site **B** becomes more strongly electron-withdrawing when a {Re(CO)$_3$Cl} fragment is coordinated to it, which is exactly consistent with the electrochemical results (above). On this basis, we argue that the delocalization of the promoted electron (Ru → **ABRe**) is facilitated by the presence of the electron-withdrawing Re complex units.[19]

In polynuclear species, a useful procedure to gauge the intercomponent electronic interaction is based on the assessment of the additive properties for the absorption spectra of the components.[3,7] In our case, with respect to the **Ru**−**AB** and **Re**−**AB** mononuclear complexes, the heteronuclear complexes actually share the **AB** ligand; thus this approach cannot strictly be applied. In addition, as discussed above, the Re-based reference model with the metal coordinated at the B site is not available.[29] On the other hand, from previous studies performed on the dinuclear **Ru**−**ABRe** and **ReAB**−**Ru** complexes (where the Ru and Re centers are coordinated to the A site of the **AB** ligand, respectively), it is already known that the intercomponent interaction is sufficiently strong to allow fast and complete Re(B) → Ru(A) and Ru(B) → Re(A) energy transfer, respectively, even if the two chromophores keep their electronic identity to a certain degree.

Figure 5 shows the absorption spectra of **Re**−**AB**, **Ru**−**AB$_3$**, and **Ru**−**ABRe$_3$** (room temperature). From this one can see that for **Ru**−**ABRe$_3$** the prominent shoulder around 380 nm is related to the Re → **BA** transition, responsible for the absorption of *ca*. 60% of the light at this wavelength, while use of light at 465 nm leads to selective excitation of the Ru-based chromophore. Similarly, for the other heterometallic complexes it is possible to excite selectively the Ru-based chromophore (λ_{exc} = 465 nm) or to excite both the Ru- and Re-based groups together (λ_{exc} = 380 nm).

Luminescence Properties. Table 5 lists the uncorrected luminescence band maxima, quantum yields, and emission lifetimes obtained in degassed solutions at room temperature and in frozen media at 77 K by employing λ_{exc} = 465 nm. It also lists the radiative and nonradiative rate constants, k_r and k_{nr} respectively, for deactivation of the luminescent excited states as calculated in accord with eq 2.

$$k_r = \Phi/\tau \tag{2a}$$

$$k_{nr} = 1/\tau - k_r \tag{2b}$$

Figure 6 shows the luminescence spectra of the **Re**−**AB**, **Ru**−**AB$_3$**, and **Ru**−**ABRe$_3$** complexes at 295 K, as obtained from isoabsorbing solutions at λ_{exc} = 380 nm. The luminescence properties for the two series of complexes **Ru**−**AB$_n$** and **Ru**−**ABRe$_n$** are discussed separately below.

Ru−**AB$_n$ Series.** The room temperature luminescence band maxima are nearly identical for these complexes (Table 5). In contrast, the luminescence lifetime and quantum yield values decrease for sequential substitution of **AB** for bpy ligands. In principle, for this series of complexes the lowest excited level could be of Ru → bpy or Ru → **AB** CT electronic configuration. Consistent with the absorption properties (see above) and with previously obtained results[21] and because of electronic delocalization, the lowest-lying level is thought to be the formally triplet Ru → **AB** CT state. The changes in the luminescence quantum yields and lifetimes in the series are more difficult to interpret. One explanation might be based on steric hindrance of **AB** quaterpyridine resulting in a slightly lower ligand field and, in turn, lowering the metal-centered (MC) levels. Thus, as shown by previous investigations,[12,30] a small MLCT−MC energy gap can cause enhancement of the radiationless deactivation of the luminescent level. In agreement with this, the radiationless rates k_{nr} reported in Table 5 for the series **Ru**−**AB$_n$** increase with the number of **AB** ligands in the complexes.

Ru−**ABRe$_n$ Series.** These heteronuclear complexes contain the chromophores $[Ru(bpy)_n(AB)_{3-n}]^{2+}$ and $[(AB)Re(CO)_3Cl]$ with the Ru and Re centers coordinated at the A and B sites of **AB** quaterpyridine, respectively. On this basis, the complexes of the **Ru**−**AB$_n$** series (discussed above) are satisfactory component models for discussing the spectroscopic properties of the heteronuclear complexes. On the contrary, the available **Re**−**AB** complex, where the metal center is coordinated to the A site of **AB**, is not a fully satisfactory model because coordination at A or B results in different spectroscopic properties.[22] The effect of coordinating a metal center at A or B sites of **AB** can be evaluated by comparing the luminescence properties of $[(bpy)_2Ru-AB-Os(bpy)_2]^{4+}$ (**Ru**−**AB**−**Os**, with Os coordinated at the B site) and $[(bpy)_2Os-AB-Ru(bpy)_2]^{4+}$ (**Os**−**AB**−**Ru**, with Os coordinated at the A site) dinuclear complexes.[21] For both **Ru**−**AB**−**Os** and **Os**−**AB**−**Ru** complexes, the lowest-lying luminescent level involves the Os center being of Os → **BA** and Os → **AB** CT nature, with λ_{max} = 756 and 808 nm, respectively. Thus, in **Ru**−**AB**−**Os** the Os-based luminescent CT level (at site B) is *ca*. 600 cm^{-1} higher in energy with respect to its positional isomer, **Os**−**AB**−**Ru**, where the Os-based emission occurs from site A. Turning to the presently investigated complexes, the reported emission band maximum for the model complex **Re**−**AB**, λ_{max} = 616 nm (Table 5,

(30) (a) Barigelletti, F.; De Cola, L.; Juris, A. *Gazz. Chim. Ital.* **1990**, *120*, 545. (b) Fabian, R. H.; Klassen, D. M.; Sonntag, R. W. *Inorg. Chem.* **1980**, *19*, 1977. (c) Kelly, J. M.; Long, C.; O'Connell, C. M.; Vos, J. G.; Tinnemans, A. H. A. *Inorg. Chem.* **1983**, *22*, 2818. (d) Constable, E. C.; Hannon, M. J.; Cargill Thompson, A. M. W.; Tocher, D. A.; Walker, J. V. *Supramol. Chem.* **1993**, *2*, 243.

Table 5. Luminescence and Photophysical Data for the New Complexes[a]

	295 K [b]						77 K	
complex	λ_{max}, nm	τ, ns	$\Phi \times 10^2$	$k_r \times 10^{-4}$, s^{-1}	$k_{nr} \times 10^{-5}$, s^{-1}	$k_q^{O_2} \times 10^{-5}$, s^{-1}	λ_{max}, nm	τ, μs
Ru−AB	610	320 (250)[c]	2.8	8.6	30.0	8.8	602	5.2
Ru−AB$_2$	612	220 (180)	1.8	8.0	44.0	10.1	604	5.0
Ru−AB$_3$	612	160 (140)	1.0	6.3	62.0	8.9	606	4.8
Ru−ABRe	622	1010 (650)	11.0	10.9	8.8	5.5	607	4.7
Ru−ABRe$_2$	612	720 (560)	9.9	13.8	12.5	4.0	606	4.8
Ru−ABRe$_3$	612	490 (450)	6.0	12.2	19.2	1.8	606	4.9
Re−AB[d]	616	22	0.15				535	3.2
$[Ru(bpy)_3]^{2+}$[e]	608	170	1.5				582	5.0

[a] In DMF/CH_2Cl_2 solvent (9:1, v/v), the band maxima are from uncorrected spectra; $\lambda_{exc} = 465$ nm unless otherwise stated. [b] Deaerated samples unless otherwise stated. [c] Values in parentheses are for air-equilibrated samples. [d] $\lambda_{exc} = 380$ nm, air-equilibrated sample. [e] Air-equilibrated sample, acetonitrile solvent, ref 17b.

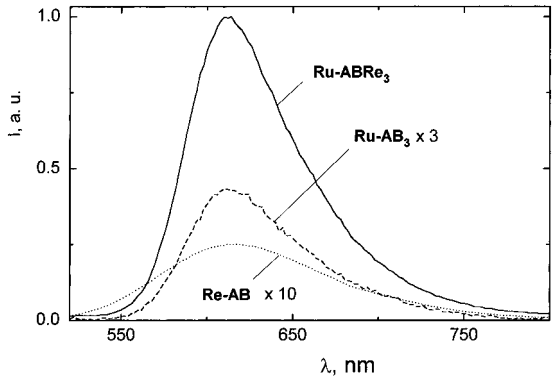

Figure 6. Uncorrected luminescence spectra at 295 K for the **Re−AB**, **Ru−AB$_3$**, and **Ru−ABRe$_3$** complexes as obtained from isoabsorbing solutions at $\lambda_{exc} = 380$ nm; the intensities are scaled as indicated.

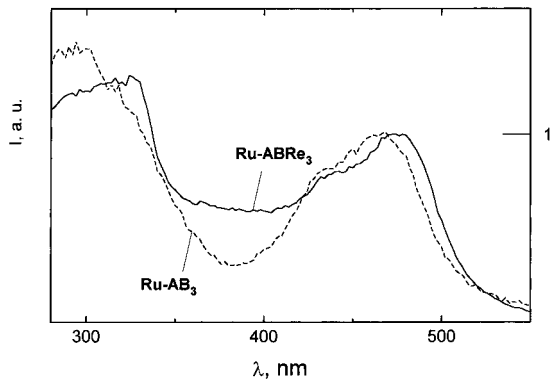

Figure 7. Normalized excitation spectra for **Ru−AB$_3$** and **Ru−ABRe$_3$** complexes.

equivalent to 16 230 cm^{-1}), pertains to an energy level of Re → **AB** CT electronic configuration. For the **Ru−ABRe$_n$** series, where only Re → **BA** CT levels are expected, one can reasonably estimate that the lowest-lying Re-based CT level is placed around 16 800 cm^{-1}, corresponding to 595 nm. In conclusion, for this series of complexes the lowest-lying energy level is expected to be of Ru → **AB** CT nature in all cases.

Table 5 lists luminescence properties obtained by using irradiation at 465 nm, resulting in selective excitation of the Ru-based chromophore. The room temperature band maxima occur at 622 nm for the dinuclear complex (where there is just one Re-containing unit, **Re**) and at 612 nm for the trinuclear (**Re$_2$**) and the tetranuclear (**Re$_3$**) complexes. As one can see from Table 5, the lifetime and quantum yield values for the Re-based emission of **Re−AB** ($\lambda_{exc} = 380$ nm, $\Phi = 1.5 \times 10^{-3}$, $\tau = 22$ ns) are quite different from those observed for the **Ru−AB$_n$** and **Ru−ABRe$_n$** complexes ($\lambda_{exc} = 465$ nm, $\Phi = 0.01-0.1$, $\tau = 160-1010$ ns). Notice that, as discussed above, for the hypothetical **Re−BA** complex the luminescence band maximum would be expected to peak at higher energy than for **Ru−AB**.

We assign the luminescence as Ru-centered in the **Ru−ABRe$_n$** complexes, on the basis of comparison of their luminescence properties with those of the **Ru−AB$_n$** and **Re−AB** complexes. For instance, by irradiation at 465 or 380 nm of a sample of **Ru−ABRe$_3$** one obtains selective excitation of the Ru-based chromophore or excitation of both Ru- and Re-based chromophores (in a 0.4:0.6 ratio, respectively, as estimated from the absorption spectra of Figure 4). Comparison of the luminescence properties under both excitation conditions shows that the luminescence intensity profiles overlap and that the luminescence lifetime and quantum yield are practically identical ($\tau = 450$ and 460 ns, and $\Phi = 0.06$ and 0.062, for $\lambda_{exc} = 465$ and 380 nm, respectively). Also, there is no evidence for a dual exponential decay that would occur if a mixture of Ru- and Re-based emission were occurring. Both of these facts indicate that the emission is occurring from a single metal center irrespective of which chromophore absorbs the excitation radiation. In addition, (i) comparison of the excitation spectra for **Ru−AB$_3$** and **Ru−ABRe$_3$** (Figure 7) shows that the light energy absorbed at 380 nm by the Re-based components is emitted by the Ru-based component, so providing evidence for the occurrence of a fast Re → Ru energy transfer step,[22] and (ii) for $\lambda_{exc} = 380$ nm, careful inspection on the blue side region of the luminescence spectrum does not show any Re-based contribution, consistent with complete (within experimental uncertainty) quenching of the Re-based luminescence.

These results all indicate that, for the **Ru−ABRe$_3$** complex, complete Re → Ru energy conversion takes place, consistent with the emission being of Ru-based nature, independent of the excitation wavelength. Consideration of the intrinsic deactivation rate of the Re-based donor allows estimation of the energy transfer rate as $k_{en} \geq 5 \times 10^8$ s^{-1}. The same conclusions are found to hold for **Ru−ABRe** and **Ru−ABRe$_2$**.

Discussion

Electronic Properties of the Ru-Based Chromophore. These heteronuclear complexes exhibit larger luminescence intensities and longer lifetimes with respect to the mononuclear **Ru−AB$_n$** counterparts. From the luminescence data (Table 5) we can see that this effect is due to a remarkable decrease of the radiationless rate k_{nr}. Thus, for the **Ru−ABRe$_n$** complexes, the presence of the Re-based chromophore(s) has beneficial consequences because it depresses the role of radiationless paths in deactivating the Ru-based luminescent excited state. This may be related to the fact that coordination of a second metal ion [*i.e.*, of the $Re(CO)_3Cl$ group] at the B site results in conformational rearrangements of the **AB** ligand. As discussed above, in the complexes examined the ruthenium center is

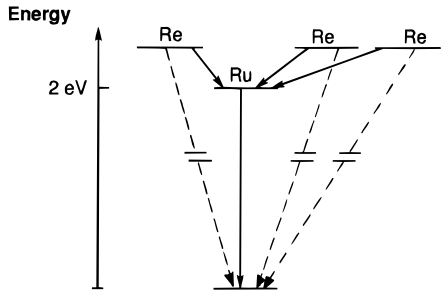

Figure 8. Schematic energy level diagram for the lowest-lying Ru- and Re-centered excited levels of the **Ru**−**ABRe$_3$** complex.

coordinated to the less hindered A chelating site while the B site either is free (**Ru**−**AB$_n$** series) or is subsequently coordinated (**Ru**−**ABRe$_n$** series).

Luminescence Quenching by O_2. In order to address quenching effects by O_2 dissolved in the solvent we have performed photophysical measurements of air-equilibrated samples and obtained the quenching rates, $k_q^{O_2}$, by using eq 3.

$$k_q^{O_2} = \frac{1}{\tau_{O_2}} - \frac{1}{\tau} \qquad (3)$$

In this equation, τ_{O_2} is the luminescence lifetime value observed in air-equilibrated solvent. Results for $k_q^{O_2}$ are collected in Table 5. It is interesting to notice that, for the mononuclear **Ru**−**AB$_n$** complexes, $k_q^{O_2}$ amounts to a constant value of *ca.* 9×10^5 s^{-1}, while it reduces to 5.5, 4.0, and 1.8×10^5 s^{-1} for **Ru**−**ABRe**, **Ru**−**ABRe$_2$**, and **Ru**−**ABRe$_3$**, respectively. Therefore, the {Re(CO)$_3$Cl} groups which surround the Ru center exert a shielding effect toward quenching by O_2. This effect is most significant for the **Ru**−**ABRe$_3$** complex, where the ruthenium core is somewhat hidden by three Re-based peripheral groups (Figure 1), and therefore relates to the degree of the steric shielding of the Ru center by the bulky Re fragments which surround it.

Antenna Effect. A modest antenna effect can be seen for the heterometallic complexes based on the fact that Re → Ru energy transfer occurs for excitation with light at ≤400 nm. A pertinent energy level diagram for **Ru**−**ABRe$_3$** is depicted in Figure 8, where the energy position of the Ru-and Re-based components has been derived from the luminescence band maxima at 77 K, Table 5. According to this energy diagram, the Ru-based chromophore, being located in a central position, draws light energy from the molecular periphery. In this way an energy content of *ca*. 2.0 eV is made available for potential use by this tetranuclear complex.[31] This result might be compared with cases where the final energy collector is Os-based, as it happens for high-nuclearity Ru/Os complexes, where Ru → Os energy transfer occurs.[8,16,18] These exhibit remarkable absorption features with up to *ca.* 200 000 M^{-1} cm^{-1} in the visible region, and as a result a large amount of energy can be collected from the various light-absorbing components, which is mainly available at the Os-based centers, *i.e.*, at an energy level ≤1.5 eV.

Conclusion

The complexes **Ru**−**ABRe, Ru**−**ABRe$_2$**, and **Ru**−**ABRe$_3$** were prepared which contain one, two, or three {Re(bpy)(CO)$_3$-Cl} fragments, respectively, pendant from a {Ru(bpy)$_3$}$^{2+}$-type core. Electrochemical studies showed that these Re fragments are weakly electron-withdrawing, with the potential of the Ru(II)/Ru(III) couple becoming more positive as the number of Re substituents increases. Luminescence studies showed that in all cases Re → Ru energy transfer occurs with near-100% efficiency: for the tetranuclear complex, it is thus possible to convey a substantial portion of the electronic excitation energy from the molecular periphery to the center. It is also found that the peripheral bulky Re-containing units exert a steric shielding effect against luminescence quenching processes of the central Ru core by molecular oxygen dissolved in the solvent. The mononuclear complex [Ru(AB)(η^3-AB)Cl][PF$_6$] was characterized crystallographically and incorporates one **AB** ligand bound in a hitherto unobserved terdentate coordination mode.

Acknowledgment. We thank M. Minghetti and L. Ventura for technical assistance. This work was supported by Progetto Strategico Tecnologie Chimiche Innovative of CNR, Italy, and by the EPSRC, U.K.

Supporting Information Available: Tables of X-ray experimental details and crystallographic data, all atomic coordinates, anisotropic thermal parameters, and bond distances and angles for the crystal structure of [Ru(AB)(η^3-AB)Cl][PF$_6$]·2MeCN (10 pages). Ordering information is given on any current masthead page.

IC9615281

(31) (a) Amadelli, R.; Argazzi, R.; Bignozzi, C. A.; Scandola, F. *J. Am. Chem. Soc.* **1990**, *112*, 7099. (b) Bignozzi, C. A.; Argazzi, R.; Chiorboli, C.; Scandola, F.; Dyer, R. B.; Schoonover, J. R.; Meyer, T. J. *Inorg. Chem.* **1994**, *33*, 1652.